



ELSEVIER

Pulsed laser deposition of electronic ceramics

J.S. Horwitz, D.B. Chrisey, P.C. Dorsey, L.A. Knauss, J.M. Pond, M. Wilson,
M.S. Osofsky, S.B. Qadri, J. Caulfield, R.C.Y. Auyeung

Naval Research Laboratory, Washington, D.C. 20375, USA

Abstract

High quality thin films of electronic ceramics are currently being deposited by pulsed laser deposition (PLD) for a variety of applications. Examples of these applications include ferroelectric thin films for active microwave electronics and rare-earth doped manganite thin films for uncooled infrared focal plane arrays (IRFPAs). Single phase and oriented $\text{Sr}_x\text{Ba}_{(1-x)}\text{TiO}_3$ films have been deposited by PLD onto (100) substrates of LaAlO_3 for active microwave devices. The dielectric properties of these films has been measured using gold interdigital capacitors deposited on top of the film. A 2:1 change in the capacitance can be achieved using a 40 V bias across a 5–10 μm capacitor gap. The dissipation factor (measured at 1 MHz) depends on film composition and temperature. Rare-earth manganite ($\text{RE}_x\text{M}_{1-x}\text{MnO}_\delta$) thin films have also been deposited by PLD for use in uncooled IRFPAs. The temperature dependence of the resistivity has been measured for $\text{La}_{0.67}\text{Ca}_{0.33}\text{MnO}_3$ and $\text{La}_{0.67}\text{Sr}_{0.33}\text{MnO}_3$ thin films deposited onto LaAlO_3 substrates. Film properties depend strongly on composition and post-deposition processing conditions to vary the oxygen stoichiometry. The temperature coefficient of resistance (TCR) has been measured to be between 2 and 15%. Based on preliminary measurements, these films will increase the sensitivity of the uncooled IR detector to be comparable or greater than a cooled detector based on HgCdTe.

1. Introduction

Pulsed laser deposition (PLD) is a new physical vapor deposition technique that is making available thin films of complex multicomponent materials for the design and fabrication of advance electronic devices [1]. Single phase and epitaxial thin films can be deposited in situ, requiring no further post-processing to achieve the desired properties. Recent applications of PLD include high temperature superconductors, ferroelectrics, magnetoresistive materials and ferrites [1].

As an example, ferroelectric thin films grown by PLD are currently being explored for development of frequency agile microwave electronics [2,3]. These devices take advantage of the electric field dependence of the dielectric constant in the ferroelectric film. Tunable, high Q , low loss resonant structures can be fabricated from normal metal-ferroelectric and HTS-ferroelectric thin film multilayers. Several critical issues need to be addressed for the fabrication of ferroelectric thin films for microwave applications. These issues include the characterization of thin film properties at microwave frequencies to determine the structural properties affecting the dielectric constant, tunability, Curie temperature and dielectric losses.

$\text{Sr}_x\text{Ba}_{(1-x)}\text{TiO}_3$ (SBT) is ideally suited for the development of ferroelectric based microwave electronics. The Curie temperature of bulk SBT ranges from 30 to 400°C for x between 1 and 0, respectively [4]. The ability to control the dielectric properties in a simple way will allow prototype device structures to be easily optimized for maximum tunability and minimum loss at the desired frequency. We have investigated the growth of SBT thin films by pulsed laser deposition (PLD) and characterized the dielectric constant, loss tangent and dc field effect at frequencies from 1 MHz to 10 GHz.

A more recent application of electronic ceramics deposited by PLD has been found in rare-earth manganites films. Colossal magnetoresistance (CMR) with $R_{H=0}/\Delta R_H \sim 100000\%$ has been observed in thin films of rare earth manganites deposited by PLD [5–7]. These materials will have applications in magnetic field sensing and magnetic recording. These materials display a large temperature dependent resistivity and this property is currently being explored for the development of uncooled infrared focal plane arrays with comparable or enhanced sensitivity to cooled HgCdTe detectors. The materials currently being investigated are $\text{RE}_x\text{M}_{1-x}\text{MnO}_\delta$ ($\text{RE} = \text{La}, \text{Pr}$ and $\text{M} = \text{Ca}, \text{Ba}$ and Sr).

2. Experimental

Thin films were deposited by PLD onto single crystal substrates. The output of a short pulsed (30 ns FWHM) excimer laser operating on KrF (248 nm) was focused to an energy density of 1–2 J/cm² onto a stoichiometric target. SBT targets ($x=0-0.8$) were prepared by mixing appropriate amounts of SrTiO₃ and BaTiO₃ powders, pressing 3/4" diameter targets to 15000 pounds and then annealing overnight in flowing oxygen to a maximum temperature of 750°C. For the rare earth manganites, fully reacted, phase pure targets were prepared from the component oxides. Stoichiometric mixtures were repeatedly mixed in a mortar and pestle and then pressed into 3/4" pellets which were heated at temperatures from 1100 to 1500°C in air.

The target substrate distance was fixed at 3 cm. Films were deposited in flowing oxygen (~10 sccm) onto heated substrates (600–850°C). Substrates were attached using silver print to a stainless steel block which was heated by the output from two 360 W quartz-halogen lamps. The laser repetition rate was 5–10 Hz. Film deposition rates were ~2.5–3 Å/laser pulse on 1.0–1.5 cm² substrates. X-ray diffraction patterns were obtained using Cu K_α radiation from a rotating anode source using the standard $\theta-2\theta$ geometry.

For the interdigital capacitors on top of the SBT films, a thick Au or Ag film was deposited by e-beam evaporation through a PMMA mask to a thickness of 1–2 μm. Film properties were determined using a HP HP4284A LCR at 1 MHz and an HP 8753A network analyzer from 1 to 10 GHz. For the rare-earth-manganites, the resistance

versus temperature was measured using a standard four-point probe technique.

3. Results

3.1. Ferroelectric thin films

SBT films were found, by X-ray diffraction, to be single phase and well-oriented. Fig. 1 shows a $\theta/2\theta$ scan for $x=0.5$ which is typical of all the compositions investigated. The film is exclusively (001) oriented with a (002) ω -scan FWHM of only 0.19°. Typically, ω -scan curves for the SBT films ranged from 0.3 to 0.7° for the (002) reflection. However, for several films, the ω -scan was near or at the 1/6° resolution of the diffractometer.

Further characterization of the film structure was made using monochromatic synchrotron radiation. Fig. 2 shows the rocking curve for the SBT (002) reflection measured with synchrotron radiation of 8.0 keV at the National Synchrotron Light Source using the X-14B beam line [8]. The FWHM for SBT(002) was found to be 72 arcseconds and the substrate (LaAlO₃ (002)) to be 36 arcseconds. Although there is a large mismatch between the SBT film and the LaAlO₃ substrate (4%), the rocking curve width is comparable or better than that observed for semiconductor films grown by molecular beam epitaxy for a similar film-substrate mismatch and comparable film thickness.

The dielectric properties of the ferroelectric films have been measured at 1 MHz and 1 GHz. At 1 MHz, measurements were made as a function of temperature while cooling for several dc bias electric fields. At 1 GHz measurements were made at room temperature and 65 K

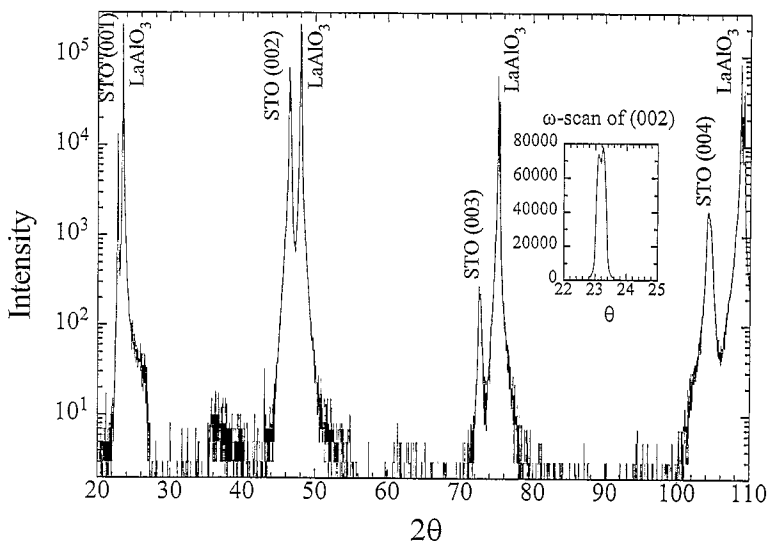


Fig. 1. X-ray diffraction pattern of SrTiO₃ (STO) grown on LaAlO₃. Inset shows an ω -scan for the (002) reflection. The splitting of the peak is the result of twinning in the substrate. The individual peaks in the ω -scan have a FWHM < 0.2°.

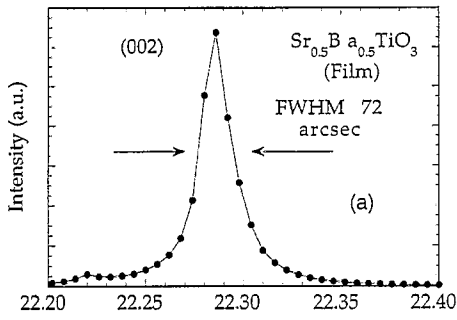


Fig. 2. X-ray rocking curve of $\text{Sr}_{0.5}\text{Ba}_{0.5}\text{TiO}_3$ (002)/ LaAlO_3 as measured on a high resolution four circle diffractometer with synchrotron radiation (8.0 keV) at Brookhaven National Laboratory.

for several dc bias electric fields. The 1 MHz measurements are shown in Fig. 3. In Fig. 3, the capacitance and dissipation factor are presented for the SrTiO_3 thin film. Several dc electric field biases were applied from 0 to 80 kV/cm (40 V applied for a gap spacing of 5 μm). The capacitance is suppressed by as much as 48% with increasing dc bias, and the peak in the capacitance (72 K with zero dc bias) shifts to higher temperatures with increasing dc bias. This behavior is typical of a ferroelectric under the influence of a dc bias [9]. There are two peaks in the dissipation factor at 95 K and 62 K which correspond closely in temperature to structural phase transitions in bulk SrTiO_3 . Bulk SrTiO_3 undergoes non-ferroelectric structural phase transitions from cubic to tetragonal at 105 K and from tetragonal to orthorhombic at 65 K [9].

In general, the thin film ferroelectric properties are different from the corresponding bulk. Previous trilayer measurements indicated that the dielectric constant of the thin film was reduced, by almost a factor of 5 for the thin film [10]. In addition, the temperature dependence of the

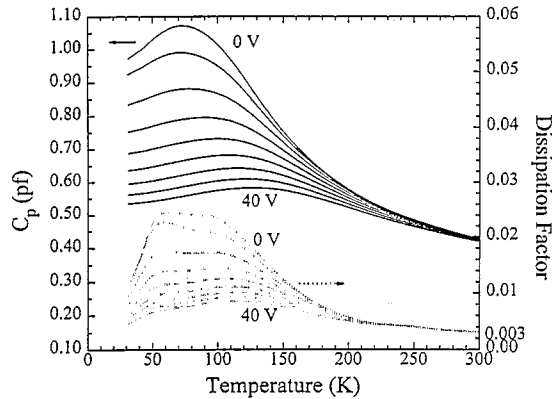


Fig. 3. Capacitance and dissipation factor for a SrTiO_3 film grown on LaAlO_3 . The measurements were made at 1 MHz with dc bias in 5 V increments up to 40 V maximum across a 5 μm gap.

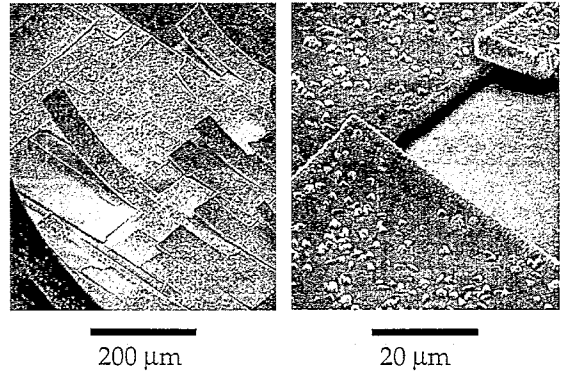


Fig. 4. Scanning electron micrograph for a 7 μm thick $\text{Sr}_{0.35}\text{Ba}_{0.65}\text{TiO}_3$ film showing cracking and delamination due to nonuniform strain.

dielectric constant is much broader than the bulk. The large lattice mismatch between the film and the substrate (4%), the enlarged lattice parameter (in the direction perpendicular to the substrate surface), and the small grain size of the film suggest that the differences between the film and the bulk may arise from strain.

The presence of strain in SBT films grown on LaAlO_3 becomes readily apparent in thick films. Fig. 4 shows an SEM photomicrograph of a $\sim 7 \mu\text{m}$ thick SBT film, $x = 0.65$. The film exhibits severe cracking and delamination. In particular, the delamination results in curved strips of SBT indicating that the strain is non-uniform perpendicular to the interface. The strain can result from several contributions: lattice mismatch, twinning in the substrate, and differences in the coefficient of thermal expansion between the film and substrate. Differences in the coefficient of thermal expansion can be ruled out as a major contribution, since the film cracked during film growth at which time the temperature was kept constant. To investigate this non-uniform strain in the thin films ($\sim 0.6 \mu\text{m}$) which typically do not crack, we measured line broadening in the X-ray diffraction peaks. Two major contributions to the broadening are non-uniform strain and crystallite size. Williamson and Hall [11] have shown that these contributions can be combined and expressed as:

$$\frac{\beta \cos \theta}{\lambda} = \frac{1}{D} + 4\varepsilon \frac{\sin \theta}{\lambda}, \quad (1)$$

where β represents the line width at half maximum, θ is the Bragg angle, ε is the strain, and λ is the wavelength of the X-rays. By plotting $(\beta \cos \theta / \lambda)$ versus $(\sin \theta / \lambda)$, one expects a straight line where the slope is proportional to strain, ε , and the intercept is proportional to the crystallite size, D . We investigated the non-uniform strain in the [001] direction by measuring the X-ray peaks for the higher order reflections off of (00 l) planes out to (004). To obtain the peak width and the Bragg angle, the lines were fit using two lorentzian peaks, one for K_{α_1} and the other

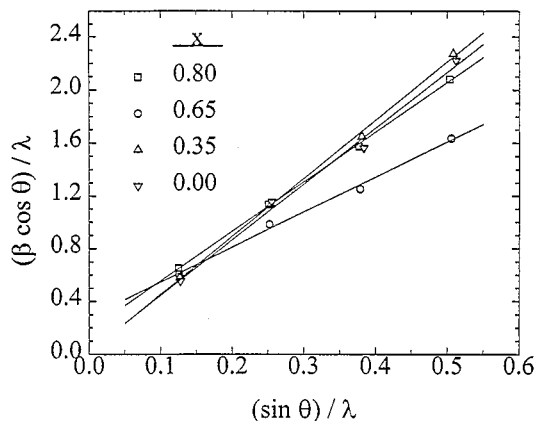


Fig. 5. Williamson and Hall [11] representation of the non-uniform strain and crystallite size contributions to the line broadening. Plotting $\beta \cos \theta / \lambda$ versus $\sin \theta / \lambda$ yields a straight line whose slope is proportional to strain and whose intercept is proportional to crystallite size.

for K_{α_2} . From the fitting parameters the Bragg angle and the peak width can be obtained. By plotting the fitting results using Eq. (1), we obtained the straight lines shown in Fig. 5. The strain and approximate crystallite size can be determined from the slope and intercept respectively. The strain is $\sim 0.1\%$ in all cases except the $x = 0.65$ composition. This is a very large strain for a ceramic material.

In an attempt to remove some of the strain, films were post-annealed in flowing oxygen at 900°C for 8 h. After annealing the as-deposited films, significant changes were observed in the dielectric properties. Fig. 6 shows the capacitance and dissipation factor as a function of temperature for the as-deposited and annealed films of SBT ($x = 0.35$). The measurements were made at 1 MHz without a dc bias electric field. The peak of the annealed film

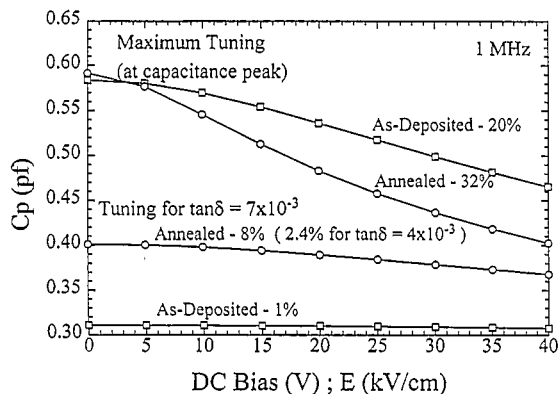


Fig. 7. Capacitance versus electric field and bias voltage temperature for $\text{Sr}_{0.35}\text{Ba}_{0.65}\text{TiO}_3$ for as-deposited and annealed films. Measurements were made at 1 MHz.

increased in temperature by 26 K which is only 10 K below the bulk transition temperature. Also, the breadth of the temperature dependence is narrower in the annealed film. When cooling the film from 375 K to 30 K, the dissipation factor in the as-deposited film increased immediately with decreasing temperature, but the annealed film had a lower dissipation factor at high temperatures which did not increase until the temperature was closer to the transition temperature. The temperature at which the dissipation factor was maximized also shifted closer to the capacitance peak after annealing.

Significant improvements in device performance can be achieved by post-annealing the ferroelectric films. Fig. 7 shows the capacitance as a function of dc bias. From these results the maximum tunability is found to be 20% for the as-deposited films and 32% for the annealed films. The maximum tunability occurs at the peak where the dissipation factor is largest. A better comparison for device applications would be in a region where the losses are lowest. The lowest loss for the as-deposited film is 7×10^{-3} where the tunability is only 1%, but for the same loss tangent in the annealed film there is 8% tuning. Furthermore, the annealed film has a loss tangent as low as 4×10^{-3} where a tuning of 2.4% is still available.

3.2. Rare-earth doped manganites ($\text{RE}_x\text{M}_{1-x}\text{MnO}_\delta$)

Recently, extremely large magnetoresistance ($R_{H=0}/\Delta R_H$) has been discovered in thin films of rare earth substituted manganites, $\text{RE}_x\text{M}_{1-x}\text{MnO}_\delta$ ($M = \text{Sr, Ba, Ca, Pb}$; $\text{RE} = \text{Pr, Nd, La}$) deposited by PLD [5–7]. Annealing of these films for a short period of time in oxygen results in magnetoresistance values exceeding 100000% at 77 K and 2 T. This new magnetoresistance regime is called colossal magnetoresistance (CMR). Further annealing of these films results in a decrease in the magnetoresistance. In addition, bulk, polycrystalline materials and single crystals of rare earth substituted lanthanum manganites only show a mod-

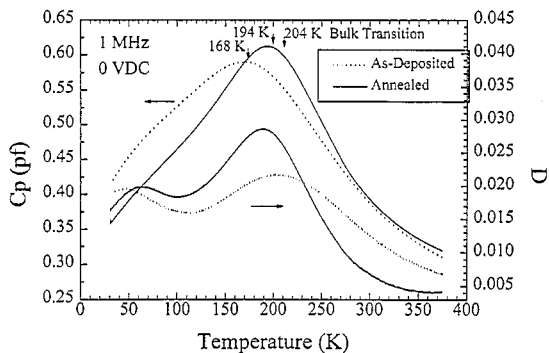


Fig. 6. Capacitance and dissipation factor versus temperature for $\text{Sr}_{0.35}\text{Ba}_{0.65}\text{TiO}_3$ as-deposited and annealed films. Measurements were made at 1 MHz without a dc bias field.

erate magnetoresistance ($\sim 100\%$). While strain, dimensionality and morphology may play a significant role in differentiating the properties of bulk polycrystalline materials from oriented thin films, annealing of the bulk material in oxygen has been shown to result in a large variation in the Mn^{3+}/Mn^{4+} ratio.

The majority of research that is currently being done on these new materials involves developing a better understanding of the CMR effect and optimization of the magnetic properties. However, the large temperature dependence of the resistivity is being explored for use in infrared sensors based on silicon microbolometers. The detector sensitivity in IR sensors which are based on these structures, is limited by the low temperature coefficient of resistance (TCR) of the active element. Absorption of IR radiation by the bolometer is detected as a change in the resistivity of this element [12]. New materials with larger TCRs will be required for this technology to be competitive with actively cooled, semiconducting detectors. Currently, silicon microbridges are coated with a V_xO_y thin film. State-of-the-art V_xO_y has a reported -2% TCR at room temperature. Under properly optimized conditions, the rare earth doped manganites offer the possibility for dramatically improving the sensitivity of microbolometers. For a microbolometer with a coating that has a TCR of 8% , the detector sensitivity approaches that of a detector based on HgCdTe (MCT) at a significantly reduced size, weight, power consumption and cost.

$La_{0.67}Ca_{0.33}MnO_8$ coatings were deposited by PLD onto single crystal substrates of $LaAlO_3$. The structure of the $La_{0.67}Ca_{0.33}MnO_8$ films was sensitive to both the substrate deposition temperature and the oxygen pressure. X-ray diffraction spectra for $La_{0.67}Ca_{0.33}MnO_8$ films deposited at $600^\circ C$ as a function of oxygen deposition pressure are shown in Fig. 8. An analysis of the X-ray diffrac-

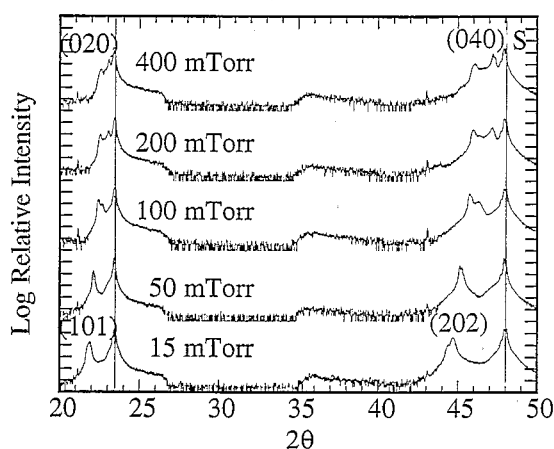


Fig. 8. X-ray diffraction patterns for $La_{0.67}Ca_{0.33}MnO_8$ thin films deposited onto (001) $LaAlO_3$. Film were deposited at a substrate temperature of $600^\circ C$ at oxygen pressures from 15 to 400 mTorr. S refers to reflections for the substrate.

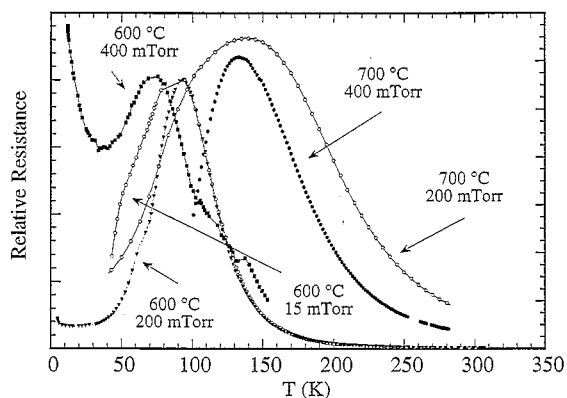


Fig. 9. $R(T)$ for $La_{0.67}Ca_{0.33}MnO_8$ thin films deposited onto (001) $LaAlO_3$ at $600^\circ C$ and $700^\circ C$ at various oxygen deposition pressures.

tion data indicates that the films are oriented and single phase with an oxygen pressure-dependent-lattice parameter. As the oxygen deposition pressure increases, the lattice parameter decreases which corresponds to an increase in δ . The diffraction peaks have been assigned to an orthorhombic structure. At low oxygen deposition pressures (15 and 50 mTorr) the film is exclusively (202) oriented. An ω -scan of the (202) peak for the film deposited at 15 mTorr had a FWHM of 0.16° which is at the $1/6^\circ$ resolution of the diffractometer. As the oxygen pressure was increased from 15 to 400 mTorr, a second orientation was observed. At 400 mTorr, the deposited film was mostly (040) oriented. An ω -scan on the (040) reflection had a broader FWHM of 0.69° .

$R(T)$ was sensitive to substrate deposition pressure and temperature as shown in Fig. 9. At $600^\circ C$, the maximum in the resistivity (T_m) varied from 73 to 93 K. The relatively

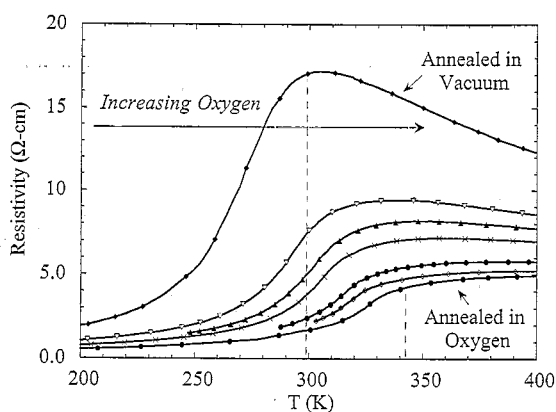


Fig. 10. $R(T)$ for $La_{0.67}Sr_{0.33}MnO_8$ thin films deposited onto (001) $LaAlO_3$ substrates. The films were first annealed at $900^\circ C$ in oxygen, then subsequently annealed at $500^\circ C$ to diffuse oxygen into or out of the film.

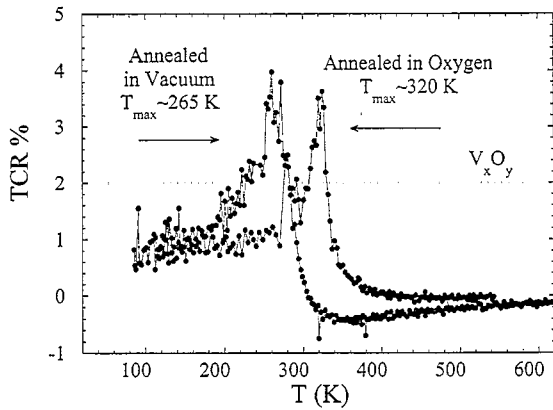


Fig. 11. %TCR for thin films of $\text{La}_{0.67}\text{Sr}_{0.33}\text{MnO}_8$ deposited onto LaAlO_3 substrates.

small change in the $R(T)$ behavior is in stark contrast to the relatively large change in oxygen stoichiometry. For films deposited at 400 mTorr, a significant difference is observed in T_m between 600 and 700°C. For the film deposited at 700°C, T_m is shifted to ~150 K. This is again in contrast to what is observed in the X-ray diffraction patterns which show the film structure to be similar.

The resistivity as a function of temperature was also sensitive to post-deposition annealing of the $\text{RE}_x\text{M}_{1-x}\text{MnO}_8$ films. Shown in Fig. 10 is $R(T)$ for a $\text{La}_{0.67}\text{Sr}_{0.33}\text{MnO}_8$ film which has been annealed in vacuum. As oxygen diffuses out of the film, the peak in the $R(T)$ curve is shifted to lower temperature. This family of curves is reproducible and the $R(T)$ maximum can be shifted back to higher temperatures by re-annealing in oxygen. For the microbolometer, the steep slope in the $R(T)$ must be near room temperature. The slope can be either be positive or negative. The $R(T)$ curves are asymmetric with the steepest slope observed in the metallic state. From

the data presented in Fig. 10, we can calculate the derivative which when normalized to the film resistance ($\times 100$) gives the %TCR (Fig. 11). The maximum TCR for this film is found to be only about 4% however, the maximum can be shifted from 265 K to 320 K.

In addition to oxygen, it is likely that strain plays a significant role in determining the maximum %TCR. As deposited films exhibit a relatively small TCR and have a TCR maximum at low temperatures. Annealing of the film in oxygen leads to an increase in the film resistivity, an increase in δ and presumably, a decrease in film strain. The $R(T)$ maximum increases and the slope of $R(T)$ increases in the metallic state, leading to an increase in TCR (Fig. 12). Continued annealing in oxygen results in a decrease in the resistance, an increase in the $R(T)$ maximum and a decrease in the TCR. In the highly annealed state, film strain has been reduced. It is likely that an optimized film for microbolometer applications will require some post deposition processing that allows for oxygen migration (positioning the steepest slope for $R(T)$ at or near room temperature) and strain.

4. Conclusion

High quality $\text{Sr}_x\text{Ba}_{(1-x)}\text{TiO}_3$ thin films have been deposited by pulsed laser deposition by pulsed laser deposition onto single crystal substrates of (100) LaAlO_3 . The deposited films exhibit a field dependent dielectric constant although the thin film properties are significantly different from the corresponding bulk material. Presumably these differences arise from strain, which is removed significantly by a post deposition anneal. The high frequency-data show that ferroelectric thin films can be used to fabricate low loss active microwave devices. Another class of electronic ceramics ($\text{RE}_x\text{M}_{1-x}\text{MnO}_8$) thin films is currently being investigated for use in IRFPAs. These materials exhibit a large temperature dependent resistivity that depends on composition (RE and M), strain and δ . A large %TCR (15%) has been observed for $\text{La}_{0.67}\text{Ca}_{0.33}\text{MnO}_8$. It should be possible to optimize these thin film to achieve a large %TCR at room temperature. Uncooled IR detectors fabricated from silicon microbridges coated with $\text{RE}_x\text{M}_{1-x}\text{MnO}_8$ thin films should have comparable or greater sensitivity than detectors based on HgCdTe .

References

- [1] D.B. Chrisey and G.K. Hubler, eds., Pulsed laser Deposition (Wiley, New York, 1994).
- [2] J.S. Horwitz, D.B. Chrisey, J.M. Pond, R.C.Y. Auyeung, C.M. Cotell, K.S. Grabowski, P.C. Dorsey and M.S. Kluskens, Integr. Ferroelectrics 8 (1995) 53.
- [3] V.K. Varadan, D.K. Gohdgaonkar, V.V. Varadan, J.F. Kelly and P. Glikerdas, Microwave J. (Jan.) 116 (1992).

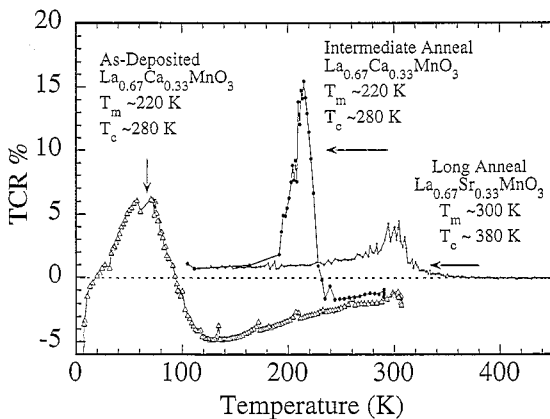


Fig. 12. %TCR for $\text{La}_{0.67}\text{Ca}_{0.33}\text{MnO}_8$ and $\text{La}_{0.67}\text{Sr}_{0.33}\text{MnO}_8$ thin films deposited onto (001) LaAlO_3 substrates.

- [4] G.A. Smolenskii and K.I. Rozachev, *Zh. Tekh. Fiz.* 24 (1954) 1751.
- [5] S. Jin, T.H. Tietel, M. McCormack, R.A. Fastnacht, R. Ramesh and L.H. Cohen, *Science* 264 (1994) 413.
- [6] M. McCormack, S. Jin, T.H. Tiefel, R.M. Flemming, J.M. Phillips and R. Ramesh, *Appl. Phys. Lett.* 64 (1994) 3015.
- [7] S. Jin, M. McCormack, T.H. Tiefel, R. Ramesh, *J. Appl. Phys.* 76 (1994) 6929.
- [8] S.B. Qadri, J.S. Horwitz, R.C.Y. Auyeung and K.S. Grabowski, *Appl. Phys. Lett.* 66 (1995) 1605.
- [9] M.E. Lines and A.M. Glass, *Principals and Applications of Ferroelectrics and Related Materials* (Oxford University Press, Oxford, 1977).
- [10] K.R. Carroll, J.M. Pond, D.B. Chrisey, J.S. Horwitz, R.E. Leuchtner, *Appl. Phys. Lett.* 62 (1993) 1845.
- [11] W.H. Hall, *Proc. Phys. Soc.* 62 (1949) 741.
- [12] R.A. Wood, B.E. Cole, C.J. Han and R.E. Higashi, *Proc. IRIS Detector I* (1993) p. 139.